Journal of Microscopy, Vol. 220, Pt 1 October 2005, pp. 20–30
Received 11 April 2005; accepted 19 July 2005

Systematic evaluation of FRAP experiments performed in a confocal laser scanning microscope

S. SEIFFERT & W. OPPERMANN
Institute of Physical Chemistry, Clausthal University of Technology, Arnold-Sommerfeld-Strasse 4, D-38678 Clausthal-Zellerfeld, Germany

Key words. Confocal laser scanning microscopy, data analysis, dimensionality of diffusion, fluorescence recovery after photobleaching, FRAP.

Summary

The diffusion coefficient as well as the dimensionality of the diffusion process can be determined by straightforward and facile data analysis, when fluorescence recovery after photobleaching (FRAP) is measured as a function of time and space by means of confocal laser scanning microscopy. Experiments representing one-dimensional diffusion from a plane source or two-dimensional diffusion from a line source are readily realized. In the data analysis, the deviations of the actual initial conditions from ideal models are consistently taken into account, so that no calibration measurements are needed. The method is applied to FRAP experiments on solutions of Rhodamine B in glycerol and aqueous suspensions of polymethyl methacrylate microspheres.

Introduction

Within the last 30 years, fluorescence recovery after photobleaching (FRAP) has become an important and versatile technique to study the dynamics in various systems, such as living cells, membranes and other biological environments. In polymer physics, the photobleaching methods are employed to investigate diffusion in macromolecular systems, particularly in networks. A review of the fundamentals of FRAP and several examples of its applications is given by Meyvis *et al.* (1999).

The FRAP technique was introduced by Peters *et al.* (1974) and first utilized quantitatively to measure diffusion coefficients by Axelrod *et al.* (1976). Its principle is to photobleach irreversibly a certain region within a fluorescently labelled sample by irradiation with a short intense light pulse. Immediately after bleaching, a highly attenuated light beam is used to measure the recovery of fluorescence inside the bleached area as a result of diffusional exchange of bleached fluorophores by unbleached molecules from the surroundings. Analysis of this process yields information about the diffusion coefficient and the fraction of mobile species.

In a common FRAP experiment, only the rate of recovery of the fluorescence intensity within some preselected area is measured. Performing the experiment in a confocal laser scanning microscope (CLSM) reveals such information with high spatial resolution. Although this fact was referred to in some papers (Salmon *et al.*, 1984; Kubitscheck *et al.*, 1994; Cheng *et al.*, 2002; Ross & Fygenson, 2003), it has not been pointed out that major advantages with regard to data evaluation can be drawn from this.

Here we show that the diffusion coefficient can readily be obtained without any calibration measurement. Furthermore, the dimensionality of the diffusion process can be extracted in an independent manner, and a comparison of the different ways to analyse the data provides a sensitive check for consistency and margins of error. We discuss the fundamentals of the approach, describe the procedure in detail, and present some experimental results of FRAP measurements on solutions of Rhodamine B in glycerol and on aqueous suspensions of polymethyl methacrylate (PMMA) microspheres to demonstrate that reliable data are obtained.

Theoretical outline

Fundamentals

Any FRAP experiment makes use of the diffusion equation, which is also known as Fick's second law. For the one-dimensional (1D) case, when diffusion occurs in the x-direction only, it is given by

$$\frac{\partial C}{\partial t} = D\frac{\partial^2 C}{\partial x^2}. \tag{1}$$

The corresponding differential equations for the 2D and 3D are

$$\frac{\partial C}{\partial t} = D\left(\frac{\partial^2 C}{\partial x^2} + \frac{\partial^2 C}{\partial y^2}\right) \tag{2}$$

Correspondence to: Mr Sebastian Seiffert. Tel.: +49 5323 72 3642; fax: +49 5323 72 2863; e-mail: sebastian.seiffert@tu-clausthal.de

and

$$\frac{\partial C}{\partial t} = D\left(\frac{\partial^2 C}{\partial x^2} + \frac{\partial^2 C}{\partial y^2} + \frac{\partial^2 C}{\partial z^2}\right), \tag{3}$$

respectively (Crank, 1975). In these equations, C represents the concentration of the substance under consideration (the fluorophore), while D is the diffusion coefficient. All these equations can be expressed in terms of vector analysis as

$$\frac{\partial C}{\partial t} = div(D\ grad\ C). \tag{4}$$

They describe the diffusion in an isotropic medium for the 1D, 2D or 3D case.

Solutions to these equations can be obtained for certain initial and boundary conditions (Crank, 1975). We concentrate here on three simple cases which are relevant to FRAP experiments and the further discussion.

1 When at time $t = 0$ the substance is totally localized in a plane somewhere in an infinitely extended medium, diffusion occurs in one dimension only (normal to the plane), and the solution to Eq. (1) is

$$C(r,t) = \frac{M}{2(\pi Dt)^{1/2}} e^{\frac{-r^2}{4Dt}}. \tag{5}$$

2 When at $t = 0$ the substance forms a line source along the axis of a cylinder of infinite width, spreading occurs in two dimensions, and we obtain

$$C(r,t) = \frac{M}{4(\pi Dt)} e^{\frac{-r^2}{4Dt}}. \tag{6}$$

3 When we start out from a point source in an infinite 3D medium, the concentration profiles that develop will be spherically symmetrical according to

$$C(r,t) = \frac{M}{8(\pi Dt)^{3/2}} e^{\frac{-r^2}{4Dt}}. \tag{7}$$

In Eqs (5)–(7), r represents the generalized (radial) coordinate, M denotes the total amount of the diffusing species in the 3D case, while in the 2D or 1D case, it stands for the amount of substance per unit length or unit area, respectively. The three equations can be combined by introducing the parameter d for the diffusion dimension:

$$C(r,t) = \frac{M}{(4\pi Dt)^{d/2}} e^{\frac{-r^2}{4Dt}}. \tag{8}$$

Figure 1 shows some typical distributions of a diffusing species for these simple cases of 1D, 2D or 3D diffusion at three successive instants. The curves broaden and become shallower with increasing time. In each case, the concentration profiles are Gaussians whose full width at half maximum is $\sqrt{(2Dt)}$. The decrease of the prefactor with time depends on the dimensionality: the higher the diffusion dimension, the faster the drop of concentration at $r = 0$.

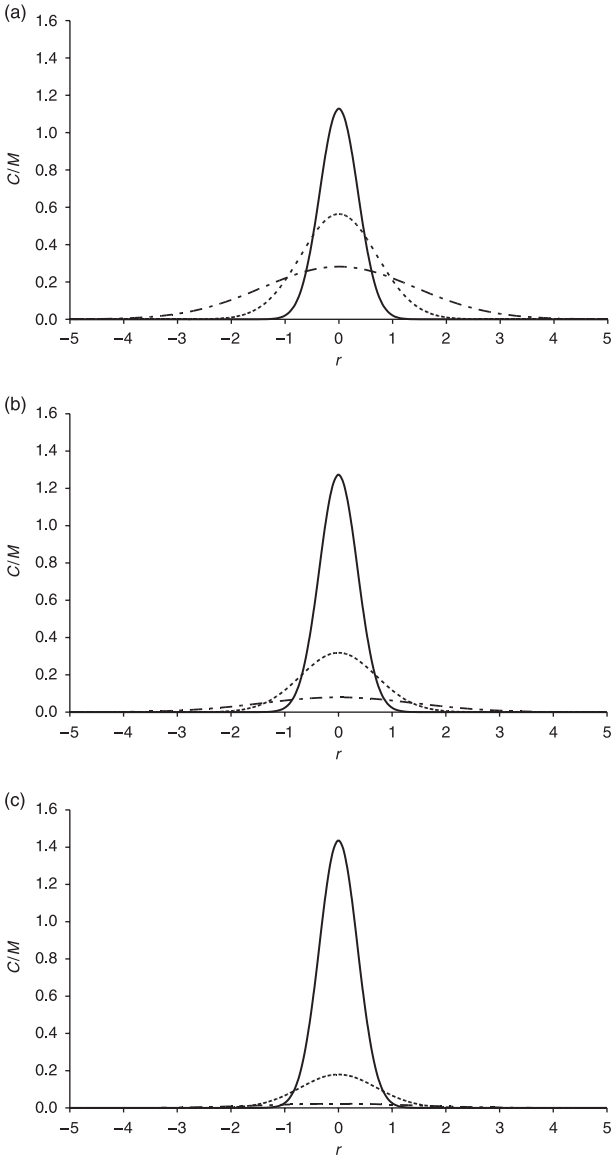

Fig. 1. Concentration profiles for simple (a) 1D, (b) 2D or (c) 3D diffusion at three distinct moments: $Dt = 1/16$ (solid line), $Dt = 1/4$ (dotted line) and $Dt = 1$ (dash dotted line). Adapted from Crank (1975).

If we consider FRAP processes, the situation is in essence just inversed, as bleaching takes away a certain amount of the fluorescent molecules, while the considerations above dealt with a local excess of a substance. This means no more than a change of sign combined with a baseline shift.

By utilizing a CLSM and an objective of low NA, it is readily possible to bleach geometries into the sample that correspond

closely to the cases of diffusion from a plane or a line source. Hence, the solutions to Fick's second law that were mentioned above are also applicable to FRAP processes.

In a real experiment, the initial conditions used so far to obtain exact solutions to the diffusion equation are never met perfectly. Instead of starting from a Dirac function (in one, two or three dimensions) for the concentration profile at $t = 0$, i.e. an infinitely sharp plane, line, or point source, the initial state will be characterized by some finite spatial width. Furthermore, some time is required to achieve bleaching. This means that it is not possible to define exactly the zero point of the time scale. Because in an experiment the initial conditions are only approximated, one should be aware that deviations from Eq. (8) are expected when such approximations cannot be neglected. That is the case when the diffusion occurs fast in comparison with the duration of the bleach pulse, or when concentration profiles are analysed on a length scale comparable with the spatial width of the bleaching beam.

In the following discussion, we first take up the case with ideal initial conditions. We show that analysing both the temporal and the spatial course of the concentration yields information on the diffusion coefficient and the dimensionality of diffusion without any calibration. Deviations from the ideal conditions are treated subsequently, and the problems related therewith solved. We show that even under extremely unfavourable conditions it is possible to obtain a correct diffusion coefficient. We first briefly consider classical FRAP experiments.

Classical FRAP experiments and recent developments

FRAP experiments carried out in standard fluorescence microscopes or similar set-ups generally proceed according to the following routine. A light pulse of high intensity is used to destroy fluorescent molecules in a small region of interest (spot). Immediately thereafter, the recovery of fluorescence inside the bleached spot due to diffusion of unbleached molecules from the surroundings is measured by means of a highly attenuated light beam. The process is quantified by the integral fluorescence intensity in the spot area. Analysis of the rate of recovery yields information about the diffusion coefficient.

The first suggestion for a quantitative treatment of FRAP experiments was given by Axelrod *et al.* (1976). They derived equations that can be used to fit an experimental recovery curve to a theoretical one. These equations are based on the assumptions that (i) fluorescence recovery (in the absence of any flow) is the result of pure 2D diffusion, (ii) a laser beam having a Gaussian or circular intensity profile is used for bleaching and detection, (iii) photobleaching occurs as an irreversible first-order reaction and (iv) the duration of the bleaching pulse is short compared with the characteristic time for recovery. A calculation of the absolute value of D requires knowledge of the beam size and profile, and hence a calibration is necessary.

In the last 20 years, several authors have developed similar approaches (Soumpasis, 1983; Lopez *et al.*, 1988; Gordon *et al.*, 1995) for 2D diffusion. By and large, they added improvement to the data evaluation or the mathematical modelling. Recently, Braeckmans *et al.* (2003) pointed out that the use of a CLSM enabled much better control of the bleaching geometry. They also expanded the model to the 3D case. Kubitscheck *et al.* (1998) derived an alternative way to determine the diffusion coefficient for the case of 3D diffusion based on numerical simulations of the post-bleach process. In all of these approaches, however, the main emphasis was put on having well-defined initial conditions and solving the diffusion equation for that particular case. By contrast, the detection of fluorescence recovery was always based on the average intensity measured inside the spot area. By doing so, all spatial information is averaged out and lost. If one employed both the temporal and the spatial information for the data analysis, this could not only serve as a check of consistency but, furthermore, permit the unambiguous determination of the dimensionality of the diffusion process.

Only a few reports consider spatially resolved recovery data at all (Salmon *et al.*, 1984; Kubitscheck *et al.*, 1994; Cheng *et al.*, 2002; Ross & Fygenson, 2003), but only in the papers of Cheng *et al.* (2002) and Kubitscheck *et al.* (1994) is the diffusion coefficient determined from fluorescence intensity profiles. However, these approaches do not suggest the possibility to estimate the diffusion dimension.

Evaluation of spatially resolved recovery data: the ideal case

Our approach to the evaluation of FRAP data is opposite to most of the classical methods. We choose the experimental conditions for bleaching such as to ensure that the actual bleaching profile comes as close as possible to a line or plane source. The course of fluorescence recovery is followed on a length scale much greater than the width of the source. In this way we need not consider the profile of the bleaching beam, a fact that leads to considerable simplification of the mathematical treatment.

The following consideration is fully based on Eq. (8). Rewriting it for the case of a FRAP experiment yields

$$I(t,r) = I_0 - \frac{M}{(4\pi Dt)^{d/2}} \cdot e^{\frac{-r^2}{4Dt}} = I_0 - A(t) \cdot e^{\frac{-r^2}{2w^2}} \qquad (9)$$

where I represents the fluorescence intensity at position r and time t after bleaching. M now is formally a fluorescence intensity (per length or area for $d = 2$ or 1) corresponding to the amount of fluorophore destroyed by bleaching, and w is the full width at half maximum of the Gaussian function.

The quantity D appears in the prefactor and the exponent of the Gaussian function, and hence both terms can be used to determine D. Comparison of the exponential terms of Eq. (9) yields

$$w^2 = 2Dt \tag{10}$$

and therewith the possibility to determine the diffusion coefficient by plotting w^2 vs. t for a series of intensity profiles obtained from images taken during the recovery process. A straight line with slope $2D$ passing through the origin should be expected.

By contrast, we obtain an algebraic decay for the time dependence of $A(t)$:

$$A(t) = \frac{M}{(4\pi D)^{d/2}} \cdot t^{-d/2}. \tag{11}$$

Equation (11) could also be used to calculate D, provided the quantity M is known by suitable calibration. As an alternative, Eq. (11) can be written in logarithmic form:

$$\log A = -\frac{d}{2}\log t + \log\frac{M}{(4\pi D)^{d/2}} = -\frac{d}{2}\log t + K. \tag{12}$$

This means that a plot of $\log A(t)$ vs. $\log t$ should give a straight line with slope $-d/2$, thus forming the basis for the experimental determination of the dimensionality of the diffusion process.

The real case

When the results of actual experiments are analysed, it is clear that there are major deviations from the ideal predictions according to Eqs (10) and (12). First, a plot of w^2 vs. t shows an appreciable intercept instead of passing through the origin. This was also reported by Cheng *et al.* (2002) without comment. Secondly, a plot of $\log A$ vs. $\log t$ is curved and approaches a straight line with a slope according to the anticipated dimensionality only at long times. Figure 2 shows a schematic comparison of the curves expected for the ideal case and the measured curves.

The reason for these deviations is clear and has already been mentioned. The beginning of the experiment is theoretically characterized by a sharp delta pulse for bleaching. In real experiments, the bleaching takes a certain period of time. In addition, the bleaching beam has a finite width. Both deviations from the ideal case result in a shift in the experimental time scale (which starts at the scanning of the first image) compared with the ideal time scale. If the duration of the bleaching pulse were infinitely short, the spatial width of the bleaching beam would account for a broadening of the bleached pattern, which in turn could be interpreted as the result of a bleaching pulse that was infinitely narrow on the spatial scale but the bleach pattern of which was observed only after a certain period of time. By contrast, if the bleaching pulse were infinitely narrow on the spatial scale, it takes a certain period of time to obtain an adequate amount of bleaching. During that time, a diffusive broadening of the bleached pattern occurs, which again causes a temporal shift in the experimental time scale.

It is thus possible to correct for these deviations either on the time scale or on the length scale:

$$w^2 = 2Dt + w_0^2 = 2D(t + t_0) \tag{13}$$

where w_0^2 denotes the intercept in Fig. 2(b), which may be transformed into a shift of the time scale, t_0. It is important to note that this shift does not have any influence on the determination of the diffusion coefficient, as D is derived from the slope of the line. However, it greatly affects the course of $\log A$ vs. $\log t$. For a correct estimate of the diffusion dimension, it is absolutely necessary to apply the correct time shift t_0. Fortunately, there are two criteria which may be used to find it and which have to be met simultaneously: t_0 has to be chosen such that the intercept of the plot of w^2 vs. $t + t_0$ is minimized and that the curvature of the plot of $\log A$ vs. $\log(t + t_0)$ is minimized as well. For convenience, we proceed in two steps. The extrapolation of the observed line in the w^2 vs. t plot to $w^2 = 0$ gives a first estimate for t_0. In the second step, a quadratic function is fitted to the $\log A$ vs. $\log(t + t_0)$ plot. Iterative variation of t_0 until the quadratic term vanishes is used for fine-tuning. The fact that both criteria are fulfilled with the same time shift t_0 is a sensitive check for consistency of the whole procedure. If the simultaneous minimization fails, deviations from purely diffusive transport must be suspected. Determination of the dimensionality of diffusion may serve as a check of the experimental conditions or as a hint to an anisotropic sample.

Realization of the concept

In this section, the evaluation procedure is comprehensively described and illustrated using FRAP experiments performed on Rhodamine B in glycerol.

As mentioned above, a CLSM allows bleaching of simple geometrical patterns like a line or a point into the confocal plane. By using an objective of low NA, this yields 3D bleaching geometries that correspond to the simple cases of 1D diffusion from a plane source or 2D diffusion from a line source. Then Eq. (9) forms the basis for the determination of the diffusion coefficient D and the dimensionality d.

In Fig. 3, some typical images are presented taken before and during FRAP experiments for the two cases mentioned above. They are for Rhodamine B in glycerol at a concentration of 0.4 g L^{-1}. These pictures show sections through the 3D sample along the confocal (x,y)-plane. Because an objective with a comparatively low NA value was used for bleaching, the bleach patterns displayed also exist along the z-axis above and below the confocal plane.

To analyse these data, the intensity profiles within the bleached areas have to be determined for each image (where each image represents a certain point in time during the fluorescence recovery process) and fitted to Eq. (9). The intensity data are averaged over different equivalent positions to reduce statistical noise. The free fitting parameters are the baseline

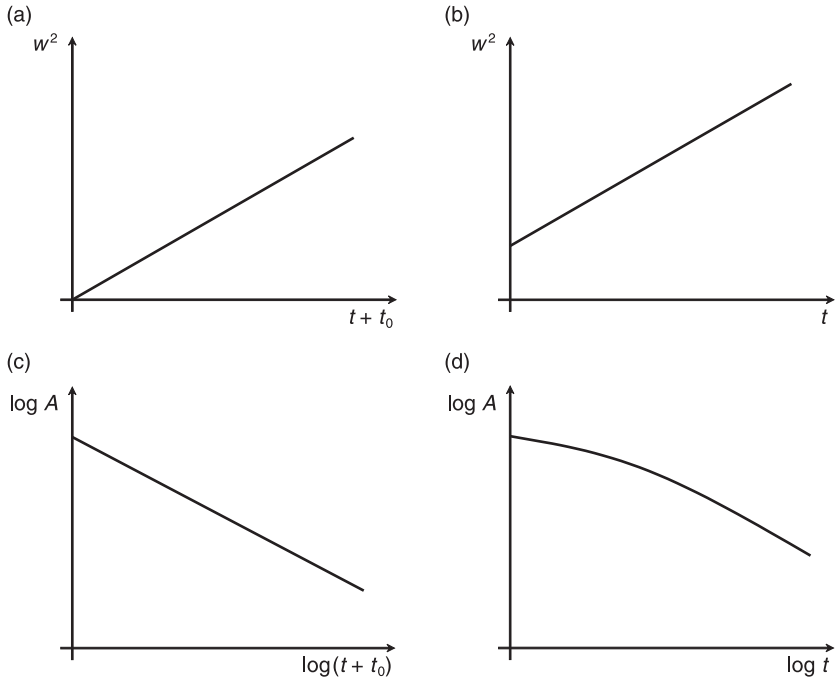

Fig. 2. Comparison of the ideal (a and c) and real (b and d) course of w^2 vs. t and of log A vs. log t (schematic). The time lag t_0 corrects for the deviations from ideality. The slope of the lines in (a) and (b) is $2D$, while it is $-d/2$ in (c).

intensity I_0, the depth of bleaching (amplitude) A and the full width at half maximum w. This yields the possibility to estimate the diffusion coefficient by plotting w^2 vs. t according to Eq. (10), while a plot of log A vs. log t should give the dimensionality d according to Eq. (12). As discussed in the preceding section, the appropriate shift of the time scale, t_0, has to be applied.

In detail, the data processing is highly automated and proceeds in the following steps.

1. Normalization. Performing a FRAP experiment on a CLSM yields a series of images of typically 512×512 pixels and 256 (colour-coded) intensity values. For automation of data analysis, a MATLAB software was written which first imports all these images and stores them as 512×512 matrices, where each entry quantifies the fluorescence intensity at that particular point by a number between 0 and 255. The image matrices corresponding to the FRAP process are then normalized to the prebleach situation by dividing each FRAP image by a mean matrix over several prebleach images. All further steps of the analysis are based on the resulting normalized FRAP matrices.

2. Averaging. Secondly, several profiles of fluorescence intensity have to be determined through the bleached region. If a point has been bleached into the confocal plane (which corresponds to 2D diffusion), it is required that the centre of the bleached spot is exactly localized. This is done by using a search algorithm (described in detail in the Appendix). Next, a mean profile of fluorescence intensity through the centre point is calculated by averaging all the intensity data within small radial intervals. In the case of bleaching a line into the confocal plane (which corresponds to 1D diffusion), the intensity data of sections running perpendicular to the bleached line are averaged. There is the option to omit some sections at the periphery of the images to avoid edge effects. As a result, an averaged (radial or linear, depending on the bleach pattern) profile of fluorescence intensity is obtained for each image and thus for each instant of the recovery process.

3. Fitting of a Gaussian function. The averaged intensity profiles for all FRAP images obtained during a recovery process are then fitted to Eq. (9) by the least-squares method. This yields a set of fit parameters for each image, namely w^2 and A, as a function of time. To demonstrate the quality of such fits, Fig. 4 shows some examples of averaged intensity profiles and the corresponding fit functions. The data belong to the images depicted in Fig. 3. The agreement is excellent, providing a sound basis for the determination of D and d.

4. Estimate of the diffusion coefficient and the dimensionality. At the end of the analysis procedure, the fitting parameter w^2 is plotted vs. t, which yields a straight line of slope $2D$. Extrapolation of this line to $w^2(t_0) = 0$ gives a first approximation for the time lag t_0. This value is later fine-tuned by plotting log A vs. log$(t + t_0)$ and fitting a quadratic function as given by Eq. (14) to the resulting curve.

$$\log A = a \cdot (\log(t + t_0))^2 + b \cdot \log(t + t_0) + c. \qquad (14)$$

By slight variation of t_0 until the coefficient a approaches zero, the correct value for the time lag t_0 can be deduced. Then, the plot of log A vs. log$(t + t_0)$ yields a straight line with slope $-d/2$.

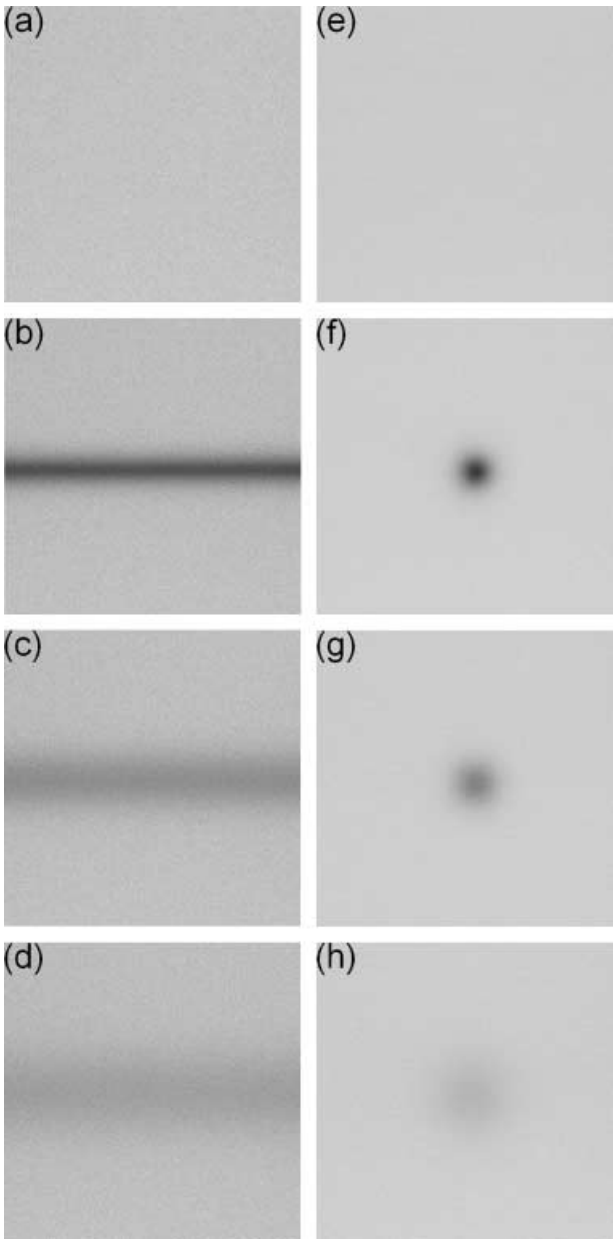

Fig. 3. Images from a series taken during FRAP experiments on Rhodamine B dissolved in glycerol ($c = 0.4\ \mathrm{g\,L^{-1}}$) for 1D diffusion after bleaching a line (left) and for 2D diffusion after bleaching a point (right) into the focal plane. Images (a) and (e) show the sample before bleaching, while images (b) and (f), (c) and (g), and (d) and (h) were taken at 1, 30 and 90 s after bleaching, respectively. The image dimensions are about $80 \times 80\ \mu\mathrm{m}^2$ for both cases.

As a result of the last step, the real FRAP experiment is transformed into the hypothetical ideal case characterized by an initial intensity profile having the form of a Dirac function. This step is discussed in detail below. It is fully implemented in the MATLAB software designed for this purpose, which is available upon request from the authors.

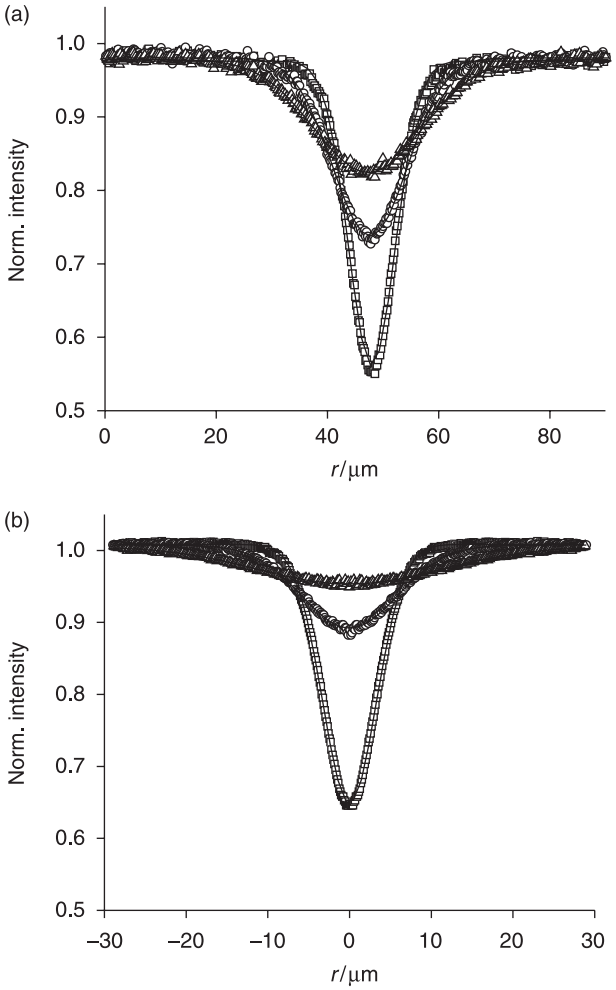

Fig. 4. Averaged intensity profiles obtained from the FRAP images shown in Fig. 3. (a) 1D diffusion, (b) 2D diffusion at 1 s (□), 30 s (○) and 90 s (△) after bleaching. The full lines are the fitted Gaussian functions.

Materials and methods

Test solutions

Rhodamine B was obtained from Sigma and dissolved in glycerol at $c = 0.4\ \mathrm{g\,L^{-1}}$. (The glycerol was not purified and may contain some water.) PMMA microspheres were obtained by an emulsion polymerization as described by Sosnowski *et al.* (1994). The resulting suspension was used as received after adding one droplet of an aqueous solution of Rhodamine B ($c = 0.4\ \mathrm{g\,L^{-1}}$) to 1 mL of the suspension. Rhodamine B is assumed to adsorb on the particle surface.

FRAP equipment

A Leica TCS SP2 CLSM was used to perform the FRAP measurements. Under a 10× DRY objective of NA = 0.3, the fluorophore was excited in the scanning mode with the 543-nm line

of the HeNe laser at 50% of its maximum intensity (which was measured to be 0.22 mW at the object level). Bleaching was accomplished by irradiation of the fluorophore with the 543-nm line of the HeNe laser and the 514-nm and the 488-nm lines of the Ar laser, each at full intensity (whereby measured intensities at the object level were 0.22, 7.0 and 6.2 mW, respectively). Further settings were: beam expander = 3, zoom = 20 (which led to an image dimension of about 80×80 μm) and line scanning speed = 800 Hz (in the scanning mode, images where taken at 1 fps) at a resolution of 512×512 pixels. For measuring the faster diffusion of the fluorescent microspheres in water, resolution was reduced to 256×256 pixels, while scanning speed was accelerated to 1000 Hz in the bidirectional scanning mode, which led to a scanning rate of 5 fps.

Ultracentrifugal analysis

Ultracentrifugal analysis was performed on a commercial analytical ultracentrifuge (OPTIMA XL-A 70, Beckmann-Coulter). Detection was performed by UV–visible absorption of the Rhodamine B-labelled PMMA suspension.

Experimental FRAP protocol

Samples for FRAP experiments were prepared by placing a droplet of each solution on a microscopy slide and placing a coverglass on top. The system was sealed with nail polish. This yields samples with a thickness of about 60 μm. The confocal plane was set to be approximately in the middle of the sample. Before bleaching, a stack of ten images was scanned to record the prebleach situation. For bleaching a point into the confocal plane (which should lead to 2D diffusion), a chosen spot in this plane was irradiated for 3 s with the laser settings mentioned above. For bleaching a line (which should yield 1D diffusion), the mode was switched into *xt*-scanning and zoom was halved to ensure that the bleached line extends over the chosen image dimensions in order to prevent side-effects. Subsequently, six images were scanned with the laser settings mentioned above. To record the post-bleach series, the mode was switched back to *xyt*-scanning and zoom was again doubled. After bleaching, a series of images was recorded to document the recovery process, with a temporal spacing of 1 s between each image for the measurements on Rhodamine B in glycerol and 0.2 s for the measurements on fluorescent microspheres at 25 °C, respectively. The time information was recorded automatically by the Leica confocal software into an information file that was accessed by our MATLAB software when analysing the data.

Data extraction and fitting

Analysis of the recorded images was automatically performed by the MATLAB software as mentioned above. All fitting results and interesting intermediate data (such as the averaged intensity profiles) were written to hard disk.

Experimental protocol of the ultracentrifugal analysis

To validate the data obtained from the FRAP-experiments, ultracentrifugal analysis measurements were taken. Estimates of the sedimentation coefficient were made from several measurements at three different rotational velocities (8000–12 000 r.p.m.) on the labelled PMMA suspension at 25 °C.

Results and discussion

To validate the concept, several FRAP experiments were performed on solutions of Rhodamine B in glycerol and on suspensions of PMMA microspheres in water.

Rhodamine B

Examples for some of the FRAP images and the corresponding intensity profiles taken from measurements on Rhodamine B in glycerol are shown in Figs 3 and 4. In Fig. 5, the fit parameter w^2 is plotted vs. (uncorrected) time for these two experiments, with one data set belonging to the line-bleaching experiment and the other to the point-bleaching experiment. The full lines are linear least-squares fits to the data. The diffusion coefficient was estimated from the slope of these lines as $D_1 = 0.56$ μm^2 s^{-1} for the 1D line-bleaching experiment and $D_2 = 0.51$ μm^2 s^{-1} for the 2D point-bleaching experiment. The results show good agreement. Furthermore, extrapolation of the straight lines yields a first approximation for the time lag t_0 of 10.8 s for line-bleaching and 6.4 s for point-bleaching.

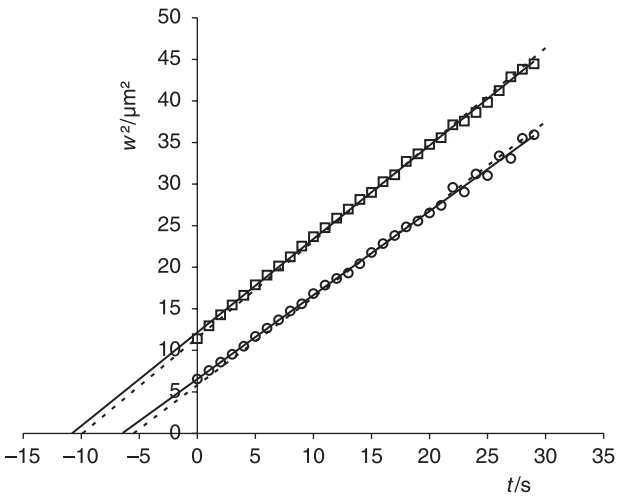

Fig. 5. w^2 vs. t plots for two examples of FRAP experiments on Rhodamine B in glycerol ($c = 0.4$ g L^{-1}): (□) line-bleaching, (○) point-bleaching experiment. The slope of the lines gives the diffusion coefficient (0.56 and 0.51 μm^2 s^{-1}, respectively), while extrapolation of the fitted lines to $w^2 = 0$ yields a first approximation for the time lag t_0 (10.8 and 6.4 s, respectively).

Table 1. Experimental results of several FRAP measurements on solutions of rhodamine B in glycerol.

	Data from extrapolation of w^2 vs. t		Data after iterative refinement		
Experiment	D ($\mu m^2 s^{-1}$)	d	D ($\mu m^2 s^{-1}$)	d	$d_{theoretical}$
Line-bleaching	0.56 ± 0.04	1.03 ± 0.11	0.58 ± 0.04	1.02 ± 0.03	1
Point-bleaching	0.56 ± 0.10	1.99 ± 0.09	0.57 ± 0.11	2.00 ± 0.09	2

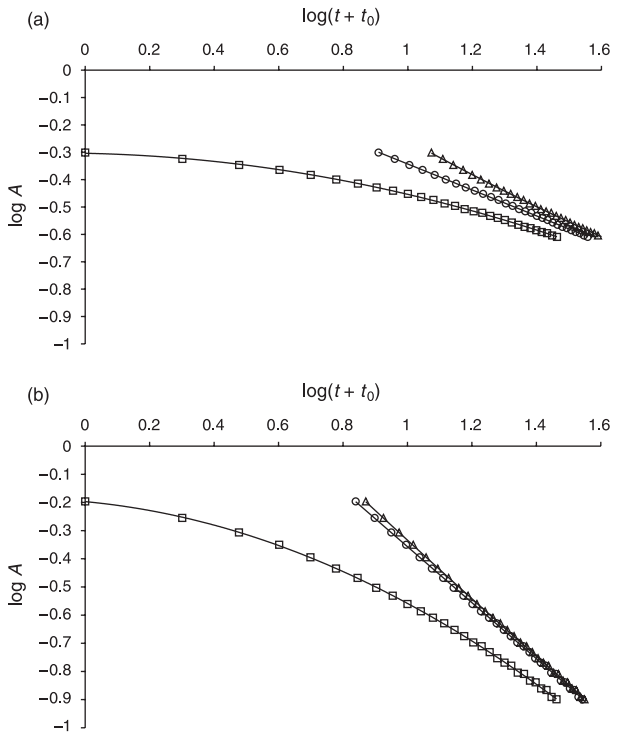

Fig. 6. Plots of log A vs. log$(t + t_0)$ for two examples of (a) line-bleaching and (b) point-bleaching experiments on Rhodamine B in glycerol. (□) Uncorrected ($t_0 = 0$), (△) after extrapolation, (○) after iteration to optimize linearity.

To estimate or check the diffusion dimension, log A is plotted vs. log$(t + t_0)$, while t_0 is fine-tuned by iteration in the manner described in the preceding sections. This procedure is visualized in Fig. 6 for the two experiments mentioned above. For comparison, plots of log A are shown vs. the logarithm of the uncorrected time, the time corrected according to Fig. 5, and the time corrected further by iteration so that the log–log plot turns out to be linear. It can be seen that the shift of the time axis is absolutely necessary to obtain the required linear course of the curve. For the point-bleaching experiment (Fig. 6b), the two lines obtained after the first and second approximation steps do not differ appreciably. The time lag t_0 is moved from 6.4 to 5.4 s. The slopes of the corresponding lines give dimensionalities of 2.05 or 1.99, respectively (theory: 2.00). For the line-bleaching experiment (Fig. 6a), the iteration has a more visible effect. Whereas t_0 is moved from 10.8 to 9.9 s, the dimensionality is estimated to be 1.15 or 0.95, respectively (theory: 1.00).

When the linear fits in Fig. 5 are forced to intersect the abscissa at the refined t_0 values, the dashed lines are obtained. These differ only marginally from the original lines, emphasizing that the refinement gives rise to just minor changes. The values for the diffusion coefficient in this case change from $D_1 = 0.56\ \mu m^2 s^{-1}$ to $D_1 = 0.58\ \mu m^2 s^{-1}$ for the (1D) line-bleaching experiment and from $D_2 = 0.51\ \mu m^2 s^{-1}$ to $D_2 = 0.53\ \mu m^2 s^{-1}$ for the (2D) point-bleaching experiment. The agreement between results achieved by different methods of evaluation and by different bleaching geometries is excellent. This is a strong argument in support of the concept.

Thus far, we have compared two simple experiments. As a check for reproducibility, each bleaching experiment was repeated five times to obtain averages of D and d as well as the of the corresponding standard deviations. The data compiled in Table 1 show that the diffusion coefficient and the diffusion dimension can be estimated to within ±10%, with point bleaching experiments showing a tendency to greater scatter.

PMMA microspheres

An aqueous suspension of monodisperse PMMA microspheres was investigated because it poses a particular challenge to FRAP measurements owing to the fact that diffusion is much faster than that of Rhodamine B in glycerol. Moreover, the size of the microspheres was determined by an independent method, and thus the absolute value of the diffusion coefficient could be checked. The microspheres had been labelled with Rhodamine B simply by adsorption of the dye from the aqueous phase.

Velocity runs in the analytical ultracentrifuge were performed to determine the particle size. The sedimentation coefficient was measured as $S = (7.1 \pm 0.3) \times 10^{-12}$ s at rotational velocities of 8000, 10 000 and 12 000 r.p.m. From this value, the radius of the particles can be calculated (Cantow, 1964; Scholtan & Lange, 1972):

$$r_p = \frac{1}{2}\sqrt{\frac{18\eta_D \ln(r/r_m)}{(\rho_P - \rho_D)\int \omega^2 dt}} = \frac{1}{2}\sqrt{\frac{18\eta_D S}{(\rho_P - \rho_D)}} \qquad (15)$$

where η_D denotes the dynamic viscosity of the dispersing medium (1.001 mPa.s), ρ_D its density (0.997 g cm^{-3}), and ρ_P

the density of the particles (1.224 g cm^{-3}, Lorenz *et al.*, 1991). Utilizing these parameters, we obtained $r_p = (11.9 \pm 0.2)$ nm. With the Stokes–Einstein equation,

$$D = \frac{kT}{6\pi\eta_D r_p} \tag{16}$$

the diffusion coefficient was calculated to be $D = (18.3 \pm 0.4)\ \mu m^2\ s^{-1}$.

FRAP experiments were performed on the same suspensions using the point-bleaching method (2D diffusion). Three repeat measurements, which were analysed according to the procedure described above in detail, gave $D = (19.3 \pm 0.5)\ \mu m^2\ s^{-1}$. The diffusion dimension was estimated to be $d = 2.03 \pm 0.10$. These results are noteworthy not only because there is good agreement between the two experimental methods with regard to D, but also because they show that the method works well even for rapidly diffusing systems. In fact, in this experiment the duration of the bleaching pulse was 3 s, while scanning was performed for only 2 s (ten images were taken in intervals of 0.2 s). It is thus corroborated that the FRAP method described here is fairly robust and suitable for handling extreme experimental conditions.

Conclusions and outlook

Performing FRAP experiments in a CLSM offers some advantages over the use of classical procedures because of two reasons: the generation of simple bleaching patterns coming close to a line or a plane source is readily possible, and the recovery process can be followed on the time scale and on the spatial scale as well. This makes data evaluation particularly facile and straightforward. Analysing the fluorescence intensity profiles obtained according to the method presented here provides not only the diffusion coefficient without any calibration measurement, but also the dimensionality of the diffusion. Because two independent criteria are used to correct the experimental time scale for the actual initial conditions, an internal check of consistency is automatically included, which would indicate any systematic errors.

The experiments performed to demonstrate the reliability of the method clearly show that the diffusion coefficient can be determined with high accuracy even under unfavourable conditions. The estimate of the dimensionality of the diffusion process agrees well with expectations. This proves that the evaluation method has a sound experimental basis.

Only slight modifications are needed to apply this method to analyse and quantify diffusion processes in anisotropic media. The principal axes of the medium would be obtained from the direction-dependent width of the Gaussian profiles, when point-bleaching experiments were performed. Utilizing a CLSM with the ability to rotate the scanning field could enable us to quantify the mobility along these directions also by line-bleaching experiments.

Acknowledgements

We thank Mr Gerald Hauser for his help concerning the development of software and methods. Dr Irina Nikiforova is gratefully acknowledged for performing the ultracentrifugal analysis measurements.

References

Axelrod, D., Koppel, D.E., Schlessinger, J., Elson, E. & Webb, W.W. (1976) Mobility measurements by analysis of fluorescence photobleaching recovery kinetics. *Biophys. J.* **16**, 1055–1069.

Braeckmans, K., Peters, L., Sanders, N.N., De Smedt, S.C. & Demeester, J. (2003) Three-dimensional fluorescence recovery after photobleaching with the confocal scanning laser microscope. *Biophys. J.* **85**, 2240–2252.

Cantow, H.-J. (1964) Zur Bestimmung von Teilchengrössenverteilungen in der Ultrazentrifuge. *Makromol. Chem.* **70**, 130–149.

Cheng, Y., Prud'homme, R.K. & Thomas, J.L. (2002) Diffusion of mesoscopic probes in aqueous polymer solutions measured by fluorescence recovery after photobleaching. *Macromolecules*, **35**, 8111–8121.

Crank, J. (1975) *The Mathematics of Diffusion*. Clarendon Press, Oxford.

Gordon, G.W., Chazotte, B., Wang, X.F. & Herman, B. (1995) Analysis of simulated and experimental fluorescence recovery after photobleaching. Data for two diffusing components. *Biophys. J.* **68**, 766–778.

Kubitscheck, U., Wedekind, P. & Peters, R. (1994) Lateral diffusion measurement at high spatial resolution by scanning microphotolysis in a confocal microscope. *Biophys. J.* **67**, 948–956.

Kubitscheck, U., Wedekind, P. & Peters, R. (1998) Three-dimensional diffusion measurements by scanning microphotolysis. *J. Microsc.* **192**, 126–138.

Lopez, A.L., Dupou, A., Altibelli, A., Trotard, J. & Tocanne, J. (1988) Fluorescence recovery after photobleaching (FRAP) experiments under conditions of uniform disk illumination. *Biophys. J.* **53**, 963–970.

Lorenz, O., Haulena, F., Reiners, A. & Roeder, D. (1991) Bestimmung der Teilchengrössenverteilung von Polymer-Dispersionen durch Ultrazentrifugation bei unterschiedlichen Wellenlängen. *D. Angew. Makromol. Chem.* **187**, 61–74.

Meyvis, T.K.L., De Smedt, S.C., Van Oostveldt, P. & Demeester, J. (1999) Fluorescence recovery after photobleaching: a versatile tool for mobility measurements in pharmaceutical research. *Pharm. Res.* **16**, 1153–1162.

Peters, R., Peters, J., Tews, K.H. & Bähr, W. (1974) A microfluorimetric study of translational diffusion in erythrocyte membranes. *Biochim. Biophys. Acta*, **367**, 282–294.

Ross, J.L. & Fygenson, D.K. (2003) Mobility of taxol in microtube bundles. *Biophys. J.* **84**, 3959–3967.

Salmon, E.D., Saxton, W.M., Leslie, R.J., Karow, M.L. & McIntosh, J.R. (1984) Diffusion coefficient of fluorescein-labeled tubulin in the cytoplasm of embryonic cells of a sea urchin: video image analysis of fluorescence redistribution after photobleaching. *J. Cell Biol.* **99**, 2157–2164.

Scholtan, W. & Lange, H. (1972) Bestimmung der Teilchengrössenverteilung von Latices mit der Ultrazentrifuge. *Kolloid-Z. U. Z. Polymere*, **250**, 782–796.

Sosnowski, S., Feng, J. & Winnik, M.A. (1994) Dye distribution in fluorescent-labeled latex prepared by emulsion polymerization. *J. Polym. Sci. A: Polym. Chem.* **32**, 1497–1505.

Soumpasis, D.M. (1983) Theoretical analysis of fluorescence photobleaching recovery experiments. *Biophys. J.* **41**, 95–97.

Appendix

Search algorithm to find the centre of the bleached spot

To find the centre of the bleached spot in FRAP images automatically, a search algorithm was written and included in our MATLAB software. We now describe its principles in detail.

As already discussed, FRAP images are present as 512×512 matrices in MATLAB, where each entry quantifies the fluorescence intensity at a particular point by a number between 0 and 255. After normalizing each image to the prebleach situation by division by a mean matrix over several prebleach images, the centre of the bleached spot is estimated in the following manner.

Each image is scanned by a test window that is moved over the image and quantifies the value of rotational symmetry for each position. If the test window is placed somewhere outside the bleached region, the rotational symmetry is lower than in the case when the test window is placed exactly over the centre of the bleached spot. To quantify the degree of rotational symmetry, the test window is duplicated and the duplicate is rotated by 90°. The difference matrix is then calculated from the rotated and non-rotated test window. If the test window is placed over the centre of the bleached spot, the rotational symmetry is high and the difference matrix contains many small entries relating to their absolute values. In the alternative case, if the test window was placed at a point within the original image with low rotational symmetry, the difference matrix shows many entries with huge absolute values. To simplify this quantification into one numerical value, all the entries of the difference matrix are squared and summed, which yields a number that we term the sum of squared differences (SSD). The lower the SSD, the higher the rotational symmetry for the present position of the test-window.

Figure 7 shows a scheme of this principle. Figure 8 presents an example of an SSD for each position of a test window of 150×150 pixels on a typical 512×512-pixel FRAP image such as that in Fig. 3(f). It can be seen that the SSD has a minimum, which marks the centre of the bleached region. In the MATLAB software, the minimum is estimated by searching the lowest entry within a fully calculated SSD matrix in a circular manner around the pixel with the lowest intensity inside the original image.

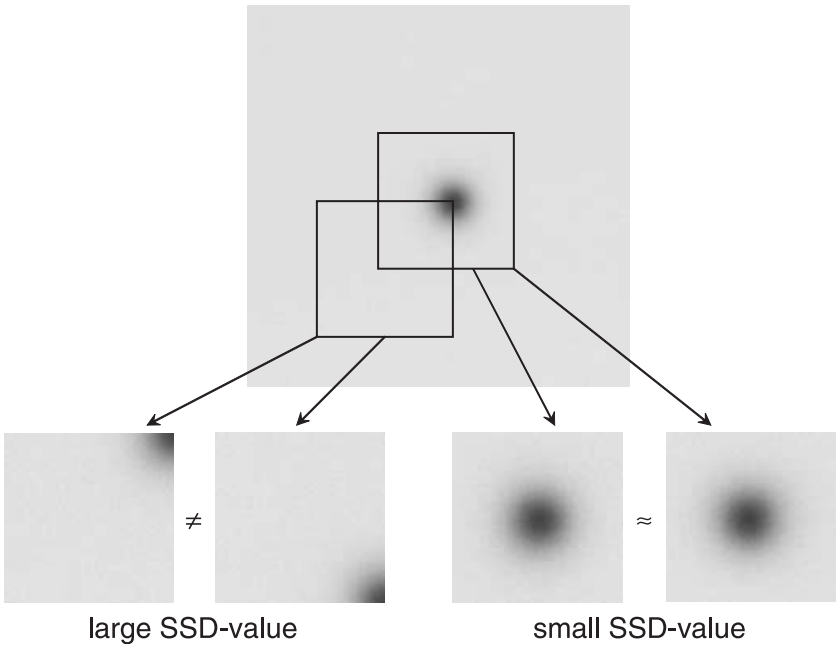

Fig. 7. Principle of the search algorithm to find the centre of the bleached spot.

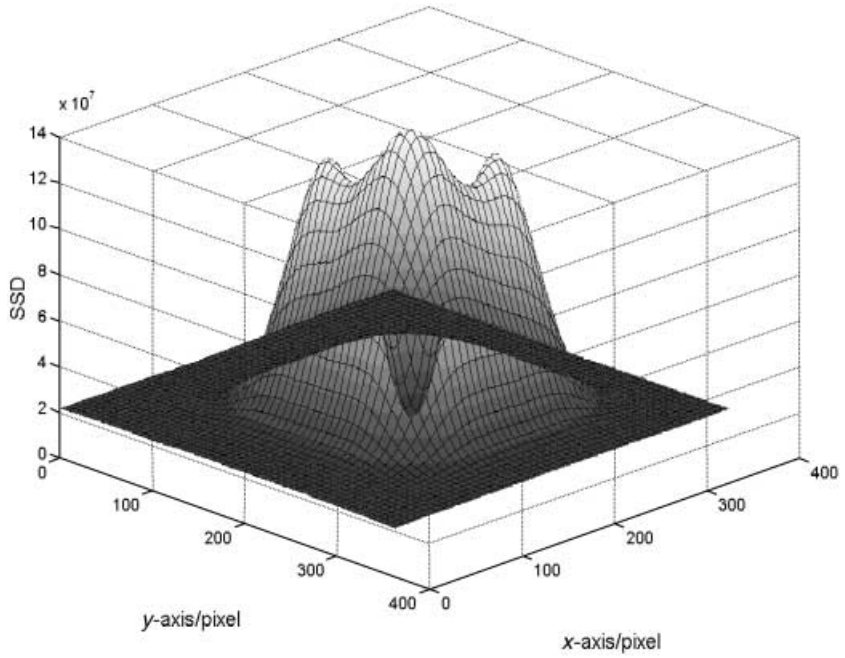

Fig. 8. Example for a plot of SSD values for each position of a test window of 150×150 pixels on a typical 512×512-pixel FRAP image.